

# NUMERICAL EXPERIMENTS PERTAINING TO WARM-FOG CLEARING<sup>1</sup>

L. RANDALL KOENIG

The Rand Corporation, Santa Monica, Calif.

## ABSTRACT

An attempt has been made quantitatively to assess the prospects for modifying warm fogs by seeding them with condensation nuclei. This has been done by calculating the time-dependent changes in the sizes and concentrations of fog droplets that are predicted by the ordinary equations of diffusion of water vapor to and from the surface of droplets. Their size, molality, and ambient water-vapor density are taken into account.

Initial conditions consist of a homogeneous volume of air of specified height and aerosol content. An external cooling rate and seed dosage are specified. The effects of various combinations of cloud height and seed properties (such as size, mass density, and rate of injection) on the metamorphosis of the fog-droplet population are examined. Usually, the cloud-forming process (in which temperature decreases with time) was allowed to continue after the completion of seeding.

It is tentatively concluded that the optimum-size seeding material is a function of the fog thickness; material smaller than about 4  $\mu\text{m}$  in diameter should be excluded, and particles 20 to 50  $\mu\text{m}$  in diameter are most suitable for seeding moderately thick ( $\sim 100$  m) clouds.

## 1. INTRODUCTION

The improvement of visibility in a fog has been one of the persistent goals of weather modification. This might be accomplished either by reducing the water content of fog or by shifting the size distribution of fog droplets toward larger droplets. The first might be achieved by warming the fog mass; the second, by modifying supercooled fog by seeding with ice-forming nuclei. In this paper, we are concerned with the problem of applying seeding techniques to natural "warm" fogs, that is, fogs composed of droplets warmer than 0°C.

Warm fogs are in equilibrium with respect to phase transition and, unlike supercooled fogs, are not amenable to artificial modification by exploitation of a latent phase instability. It has long been recognized that, in principle, one may improve visibility by seeding warm fogs with large condensation nuclei that redistribute the water content from the many small atmospheric nuclei onto the few large artificial nuclei. Problems related to the manufacture and dispersal of the seed particles have hampered the development of warm-fog seeding technology, but these appear to be on the threshold of solution. Anticipating the technical feasibility of condensation-nucleus seeding, we attempt in this paper, using numerical simulation techniques, to examine warm-fog seeding prospects and to identify factors critical to the success or failure of such ventures. The symbols used are identified in table 1.

## 2. PRINCIPLE INVOLVED IN WARM-FOG MODIFICATION BY SALT SEEDING

A natural fog forms when a parcel of air cools below its dew point. (At relative humidities greater than about 70

percent but less than 100 percent, a distinct haze forms—reducing visibility, but not enough to hinder ordinary activities.) The fog droplets form on aerosol particles, which are always present in the atmosphere.

Each aerosol particle is a latent center of condensation and is consequently a potential fog droplet. By the same token, each particle is a potential cause of reduced visibility. In fact, however, not every particle will become a

TABLE 1.—*Symbols used in this paper*

<i>B</i>	brightness, candles per square centimeter (luminance, $\text{cd cm}^{-2}$ )
<i>D</i>	mass diffusion coefficient of water vapor in air, $0.226 \text{ cm}^2 \text{ s}^{-1}$
<i>d</i>	depth of fog layer, cm
<i>e</i>	water vapor pressure, dynes per square centimeter
<i>i</i>	van't Hoff factor
<i>J</i>	mechanical equivalent of heat, $5.8 \times 10^{-8} \text{ cal cm}^{-1} \text{ } ^\circ\text{K}^{-1} \text{ s}^{-1}$
<i>K</i>	scattering-area coefficient
<i>L</i>	latent heat of condensation, $594.4 \text{ cal g}^{-1}$
<i>M</i>	molecular mass, $\text{g mol}^{-1}$
<i>m</i>	mass, g
<i>n</i>	concentration, $\text{cm}^{-3}$
<i>R</i>	universal gas constant, $8.314 \times 10^7 \text{ ergs per mole per degree Kelvin}$
<i>r</i>	radius, cm
<i>S</i>	supersaturation
<i>T</i>	absolute temperature, $^\circ\text{K}$
<i>t</i>	time, s
<i>V</i>	fall speed, $\text{cm s}^{-1}$
<i>x</i>	path length, cm
$\rho$	density, $\text{g cm}^{-3}$
$\sigma$	extinction coefficient, $\text{cm}^{-1}$
$\tau$	surface tension, 75.7 dynes per centimeter

### Subscripts

<i>c</i>	critical values
<i>j</i>	drop-size index
<i>n</i>	nucleus
<i>r</i>	on <i>z</i> , meteorological range
<i>s</i>	saturated, sky or background
<i>T<sub>a</sub></i>	at ambient temperature
<i>v</i>	virtual (see text)
<i>w</i>	water
$\lambda$	specific frequency of light
*	corrected value of <i>e</i> or <i>e<sub>s</sub></i> considering size and molality of drop
$\infty$	ambient

<sup>1</sup> This paper is a revision of Koenig (1969). That document contains a more complete discussion of the basis and derivation of the mathematical formulations employed; the present version contains information and conclusions based on additional experimentation.

fog droplet, even if the air becomes cooled below its dew point. Whether an aerosol particle becomes a fog droplet or remains a haze particle depends upon whether the droplet embryo is exposed to supersaturation greater than a critical value over a time sufficiently long for the droplet to grow beyond a critical size. The critical size and the supersaturation are both a function of the mass and the chemical composition of the nucleus. These critical values arise from the fact that the vapor pressure over a curved surface is an inverse function of the radius of curvature and the molality of a drop. For a given nucleus, the smaller the initial drop, the greater are both the curvature and the solution effects, one acting to lower the vapor pressure and the other to raise it with respect to the vapor pressure over a pure, plane surface. As a result of these opposing influences, maximum equilibrium vapor pressures over droplets occur at specific sizes that are functions of the amount and kind of soluble matter in the droplet. These are the critical sizes and critical vapor pressures for specific nuclei. The Kelvin and Raoult equations, which relate molality, drop size, and vapor pressure, may be combined and simplified, to yield approximate equations for the critical values of radius  $r_c$  and at supersaturation  $S_c$  (e.g., Fletcher 1962), namely:

$$r_c = \left[ \frac{3.91 \times 10^5 i m_n T^2}{M_n} \right]^{1/2} \quad (1)$$

and

$$S_c = \left[ \frac{1.238 \times 10^{-11} M_n}{i m_n T^3} \right]^{1/2} \quad (2)$$

Figure 1 shows curves of equilibrium vapor pressure over a drop as a function of size and nucleus content. These "Köhler" curves (Fletcher 1962) show results of the size and solution effects and critical values of size and supersaturation. Figure 2 shows the critical radius and critical supersaturation as a function of nucleus size for salt (NaCl) at 0°C.

The importance of the critical saturation may be appreciated when one realizes that only nuclei having sizes equal to or larger than the critical value corresponding to the maximum supersaturation achieved during the fog-formation process will grow into fog droplets; the remainder, restricted to sizes below their critical value, will not materially reduce the distance at which an object can be recognized and are not normally regarded as fog particles. Thus with a given size distribution of nuclei, the number of nuclei activated, and hence the fog-droplet concentration and the restriction on visibility, will be a function of the maximum supersaturation experienced during the formation of the fog. (The supersaturation itself is a function of the meteorological process responsible for formation of the fog and of the nucleus content of the air.) The fog-clearing methods investigated in this paper primarily involve the removal of water content from the fog by the fallout of large drops formed on the seeded particles. A change in the drop spectra alone is also possible. The vapor density of the foggy

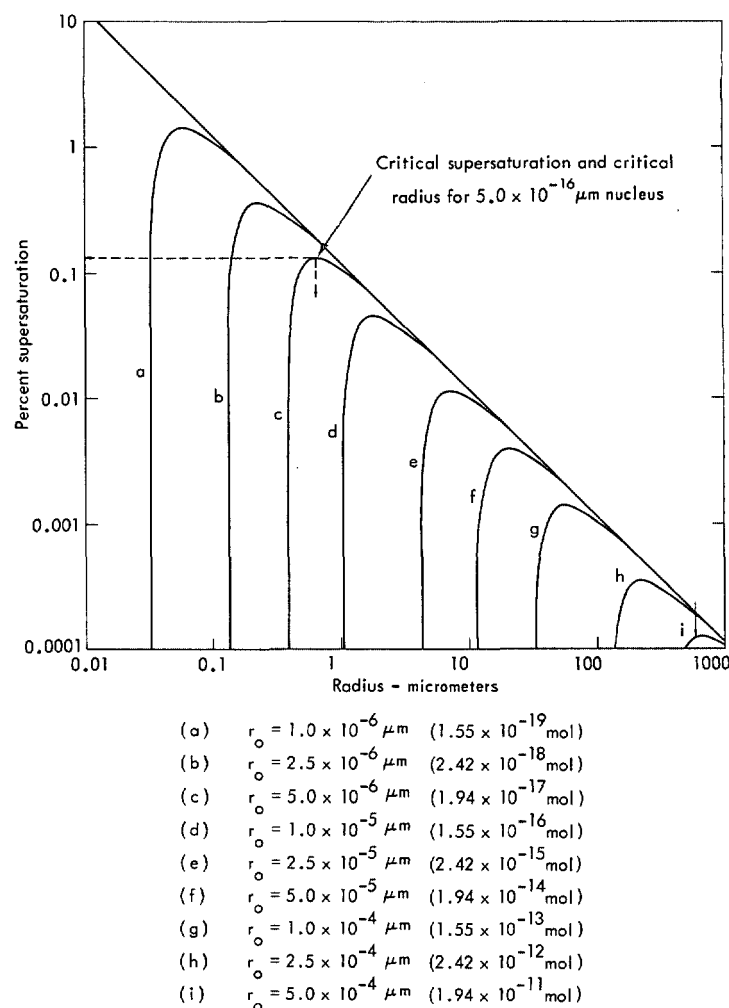


FIGURE 1.—Köhler curves for water droplets containing various quantities of sodium chloride (NaCl) particles within the size range of atmospheric condensation nuclei ( $r_0$  = dry radius of NaCl nucleus).

air is lowered below saturation long enough to evaporate some droplets below the critical size for their nucleus content. When the fog is regenerated, the vapor density is forced to remain below the maximum value achieved during the initial, natural formation of the fog; and consequently, fewer droplets grow beyond their critical radius. The result is fewer, larger drops and increased visibility. This regeneration process involves the introduction of a few additional, relatively large nuclei into the fog. The initial rapid growth of these nuclei causes the water-vapor pressure of fog to fall below saturation values, thus causing droplets having small nuclei to evaporate. It is necessary, however, to keep the water-vapor pressure below saturation for sufficient time to allow the droplets to evaporate to sizes smaller than the critical values associated with their nuclei.

When using the numerical model of liquid/vapor diffusion described in Koenig (1968) and summarized in section 3, calculations were made of the time required to evaporate drops of differing nucleus content to their

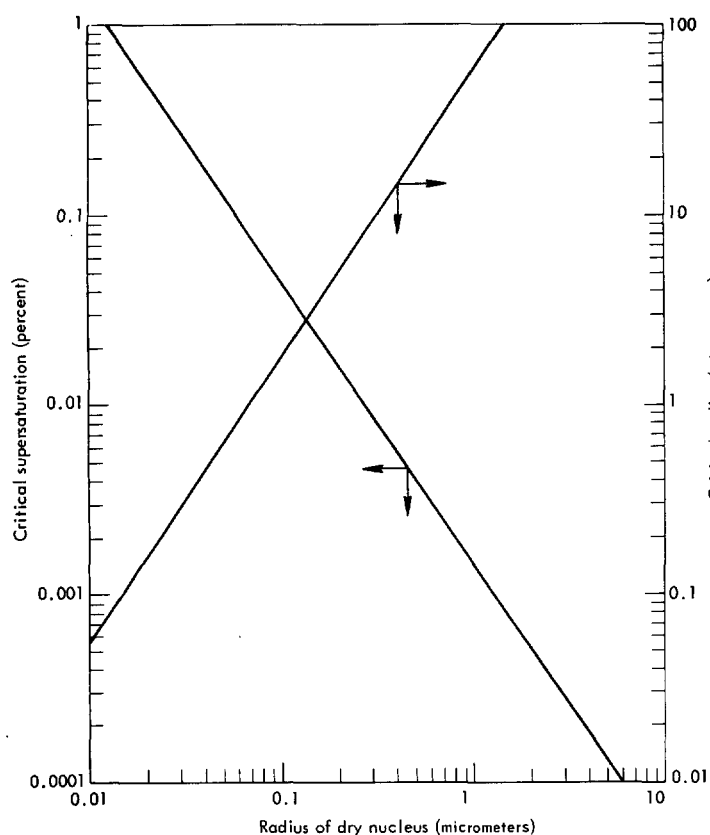


FIGURE 2.—Critical values for drop radii, and water vapor supersaturation for water droplets growing from NaCl.

equilibrium sizes at supersaturations of  $-1$  and  $-0.1$  percent (subsaturated air). Figures 3 and 4 summarize the results of these calculations and show that substantial time is required to evaporate large fog droplets having small nuclei to a size below their critical radii—even modest-sized drops require hundreds of seconds. As will be shown in section 4, if a fog-producing mechanism is active, a seeded fog does not long remain greatly subsaturated; and subsaturations of about 0.1 percent may be regarded as representative of the subsaturated period of a successfully seeded cloud if a method requiring a minimum of seeding material is used. Since rates of evaporation are approximately proportional to the degree of subsaturation, the time scale on the figures may be appropriately adjusted to suggest the evaporation history at other subsaturations.

Salt seeding lowers the water-vapor density below saturation in a volume of foggy air by providing new centers of condensation whose equilibrium vapor pressure is lower than saturation and that are numerous enough or large enough to absorb water from fog droplets in quantities sufficient to cause the droplets to evaporate below their critical radii. A measure of the ability of the seed drops to absorb water at the expense of fog particles is given by the size of the Raoult correction to the equilibrium vapor pressure over the seed droplet, or better, the virtual saturation,  $S_v$ , defined in section 3.

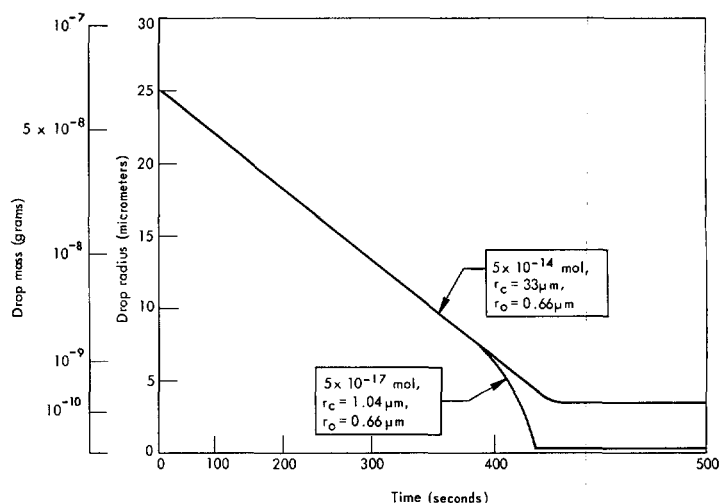


FIGURE 3.—Time required to evaporate drops containing various quantities of NaCl at supersaturation of  $-1$  percent ( $r_c$  is the critical size of the droplet, and  $r_0$  is the dry radius of the NaCl solute).

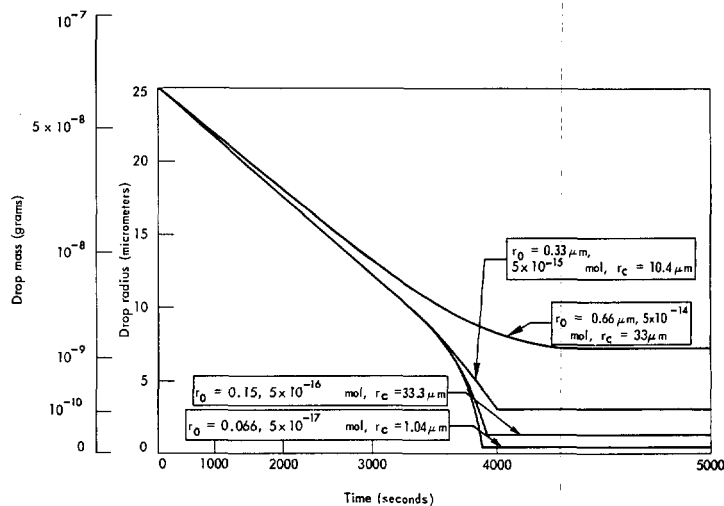


FIGURE 4.—Same as figure 3, except for  $-0.1$  percent.

When using the numerical model, calculations were made to estimate the length of time that a seed particle remains effective in gaining water at the expense of other drops in the cloud. The results are shown in figures 5 and 6, where the virtual supersaturation over the seed particle and the growth of the seed droplet are shown as functions of time and of the ambient subsaturation. It is evident that, if the seed particles must remain effective for periods of time greater than that required to evaporate fog droplets of moderate size, they must have a dry radius of at least  $0.5 \mu\text{m}$  and in fact should be considerably larger. Smaller seed particles will only increase the number of droplets in the cloud and defeat the purpose of seeding.

An excess of seed particles will produce so many new droplets that they themselves materially reduce the visibility. However, if an insufficient number of seed

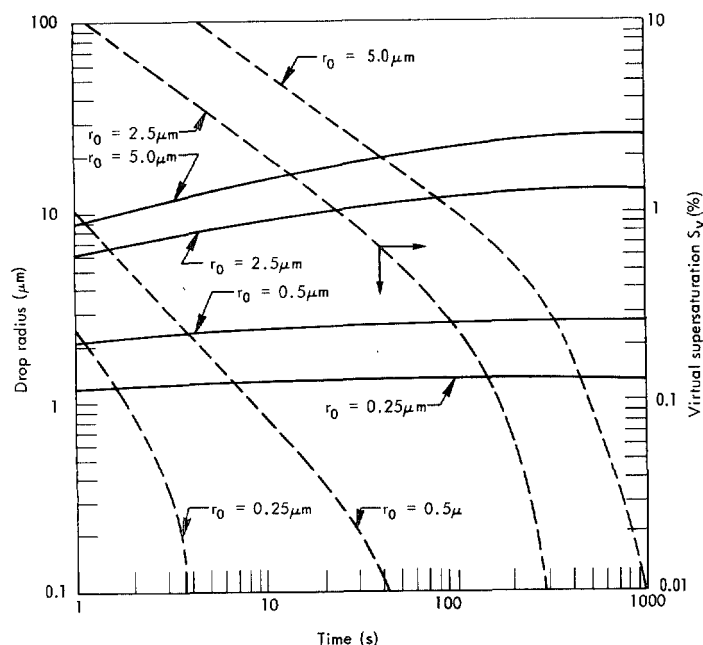


FIGURE 5.—Virtual supersaturation and drop radius as functions of time for droplets evaporating at supersaturation of  $-1$  percent and containing various quantities of NaCl seed particles ( $r_0$  is the dry radius of the NaCl solute; the relatively flat family of curves shows  $r$  versus  $t$ ).

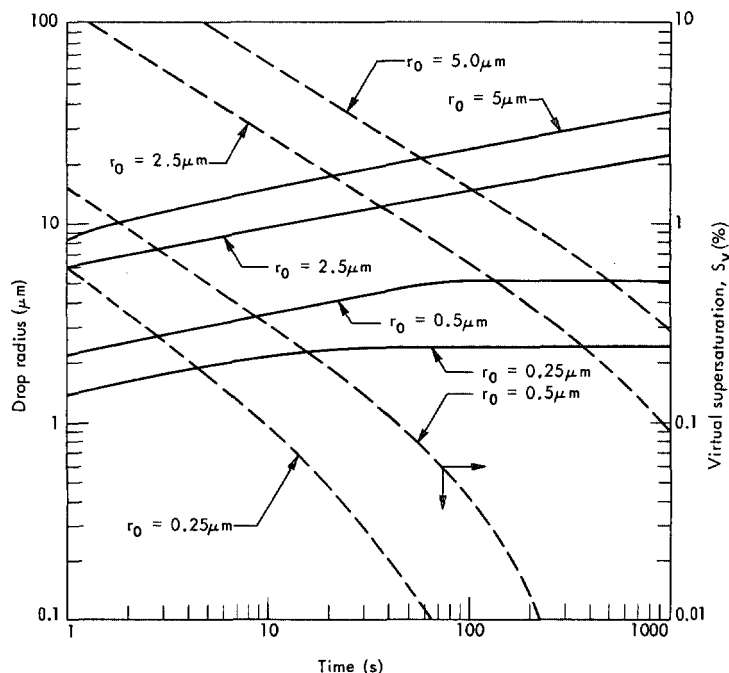


FIGURE 6.—Same as figure 5, except for  $-0.1$  percent.

particles is introduced, or if they are introduced too slowly, the ambient vapor pressure will not fall below subsaturation; and natural droplets will fail to evaporate. The same result will occur if seed particles are too small relative to the natural droplets.

We conclude that successful warm-fog seeding with condensation nuclei appears to require a technique that permits good engineering control over the size distribution, distribution rate, and ultimate concentration of the seed particles. Each of these parameters may be a function of the meteorological factors involved in the cooling process forming the fog and of the natural size distribution of condensation nuclei.

### 3. BASIS OF CALCULATIONS

#### CALCULATION OF TRANSPARENCY OF FOG

The goal of fog clearing is the improvement of an observer's ability to recognize objects. Recognition involves factors such as target characteristics and judgment, which lie outside the scope of meteorological phenomena and are thus excluded from consideration herein. For present purposes, the empirically definable term "meteorological range" will be equated with recognizability, and the measure of fog clearing achieved will be stated in terms of the improvement of meteorological range one may predict as the result of simulated seedings. Meteorological range refers to the distance at which a large, stationary object that neither reflects nor radiates visible light has an apparent brightness that is 98 percent of that in the background.

If a black object is observed in daylight at some distance from its surface, its apparent brightness will no longer be zero, since light is scattered by air molecules and aerosol particles into the line of sight of the observer. This superimposed scattered light appears to originate at the object, which thereby acquires an apparent brightness. The scattered light in the line of sight may itself be scattered and attenuated. The apparent brightness of the black object initially increases with distance; but if the distance becomes sufficiently large, the light gained by scattering into the line of sight will equal the light lost by attenuation and scattering out of the line of sight. Under this condition, brightness does not change with increasing distance, and the object will appear to have the same brightness as its background. Consequently, the contrast between object and background will vanish, and the object will cease to be visible. Middleton (1952) gives a thorough account of the physical bases for calculating meteorological range and the change in brightness contrast with distance from an object.

From Beer's law, the brightness of an object ( $B_0$ ) in relation to the sky or background brightness ( $B_s$ ) may be expressed by

$$B_0 = \int_0^\infty B_{s\lambda}(1 - e^{-\sigma_\lambda x}) d\lambda \quad (3)$$

where  $x$  is the path length through the uniform scattering volume and  $\sigma_\lambda$  is the monochromatic extinction coefficient:

$$\sigma_\lambda = n\pi K_\lambda r^2. \quad (4)$$

It is the dependence of the extinction coefficient on the concentration ( $n$ ) and radius ( $r$ ) of the droplets in the scattering volume that results in brightness being a function of the microphysical properties of fog. The

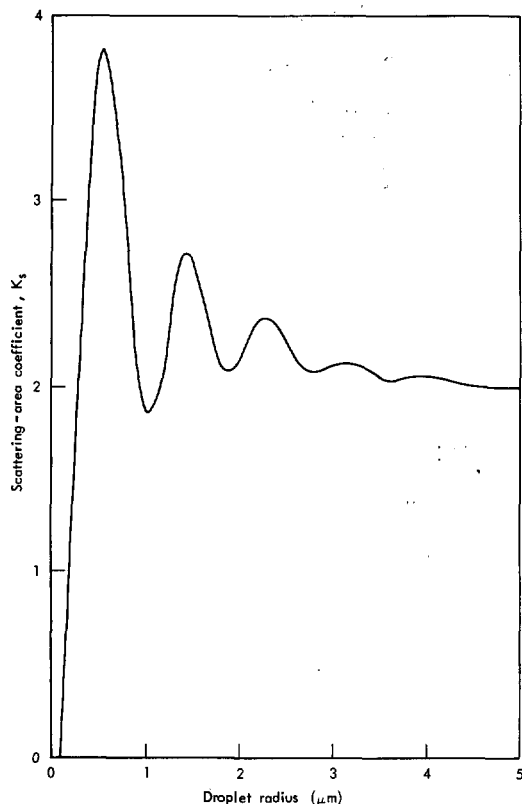


FIGURE 7.—Smoothed curve of the variation of the scattering-area coefficient with drop size, using weighted value of light based on the spectral composition of sunlight and the physiological response of the human eye.

effects of scattering and attenuation by air molecules on the extinction coefficient are not considered in this work, since these are comparatively small in fog.

The extinction coefficient is also a function of wavelength, owing to the dependence of the value of the scattering-area coefficient,  $K_s$ , on the wavelength of the light involved (e.g., table 158 of List 1966). Figure 7 is a plot of weighted mean values of the scattering-area coefficient for various drop sizes, taking into consideration the relative sensitivity of the human eye to light of various wavelengths and the relative intensity of sunlight at the top of the earth's atmosphere. For tiny drop sizes,  $K_s$  is a rapidly varying function of drop size; but as drop size increases moderately,  $K_s$  becomes nearly constant.

If  $K_s$  is considered constant, then the extinction coefficient is independent of wavelength. Using the value of  $\pm 0.02$  for the threshold brightness contrast in accordance with custom for calculating the meteorological range and using a value of 2 for  $K_s$ , one may derive the familiar equation for meteorological range from eq (3) and (4):

$$x_r = \frac{3.912}{\sum_{i=0}^{\infty} n_i K_s r_i^2} = \frac{0.6226}{\sum_{i=0}^{\infty} n_i r_i^2} \quad (5)$$

Equation (5) forms the basis of the method of calculating meteorological range used in this report. (A more detailed discussion of the basis for calculation of meteorological range used in this work may be found in Koenig 1969.)

## CALCULATION OF DROPLET EVOLUTION

The foundation for our present predictions of droplet evolution is the numerical model of condensation described by Koenig (1968). The "less complex" model described in the cited report was used in the present work. Briefly, mass-transfer rates are calculated in that model from the expression

$$\frac{dr}{dt} = \frac{[e_\infty - (e_s^*)_{T_\infty}](e_s^*)_{T_\infty}}{r \rho_w \left[ \frac{JL^2 M_w}{KRT_\infty^2} + \frac{RT_\infty}{DM_w(e_s^*)} \right]} \quad (6)$$

In this expression,  $(e_s^*)_{T_\infty}$  is the saturation vapor pressure over the drop if it is neither growing nor evaporating; it takes into account the drop's size and molality, but assumes that it is at ambient temperature. The value of  $(e_s^*)_{T_\infty}$  is found by Teten's formula (Murray 1967), modified for the effects of molality and size by Raoult and Kelvin corrections:

$$(e_s^*)_{T_\infty} = 6107.8 \exp \left[ \frac{17.269388(T_\infty - 273.16)}{(T_\infty - 35.86)} \right] \quad (\text{Teten's formula})$$

$$\times \frac{1}{1 + i m_n M_w / M_n m_w} \quad (\text{Raoult correction})$$

$$\times \exp \frac{2\tau M_w}{T_\infty R r \rho_w} \quad (\text{Kelvin correction}) \quad (7)$$

The concept of "virtual supersaturation" used in this paper is an approximate expression of the driving force causing a drop to grow, whereas "true supersaturation" is an approximate expression of the driving force causing mass transfer across a pure, flat water surface. The former is defined as:

$$S_v = \frac{e_\infty - (e_s)_{T_\infty}}{(e_s^*)_{T_\infty}} \quad (8)$$

## THE FOG MODEL

For the fog model used in this work, a spectrum of aerosol particles was input, and the growth rate of each particle was computed using eq (6). Air temperature and pressure may also be input variables; but in the work reported, pressure was always 1000 mb, and the air was initially at 24°C and at water saturation. A fixed temperature decrease with time was usually assumed; however, a draft velocity may be specified to account for the air cooling necessary for fog formation. In the former case, the feedback effects of the release of the latent heat of condensation on the air temperature may either be taken into account (to modify the assigned temperature decrease) or ignored (as was the case for all calculations used in this paper). When the draft velocity was specified, this feedback was always taken into account.

For calculating the virtual supersaturation for each nucleus,  $(e_s^*)_{T_\infty}$  was calculated; and a trial-and-error iterative procedure was used to calculate the ambient

water-vapor pressure ( $e_\infty$ ) and supersaturation. In this procedure,  $e_\infty$  was initially estimated on the basis of the temperature drop between time steps and the excess water-vapor pressure over saturation from the previous time step. The first estimate of  $e_\infty$  was used to calculate mass transfer to the entire population of droplets. The ambient supersaturation before the time step was compared with that after the time step, the temperature drop and transfer of water from the air to the droplets being considered. If the supersaturations before and after the step agreed within specified limits, it was assumed that a satisfactory value of  $e_\infty$  had been used; and the calculation was continued. This procedure resulted in a smooth change in the water-vapor density of ambient air and held the water-vapor density excess (or deficit) with respect to saturation reasonably constant between time steps, but allowed longer term changes. Euler integration was used with automatic control of time steps (0.6-s minimum, 10-s maximum). The calculations appeared to be stable and could be extended for an indefinite period of time.

Droplet fallout was incorporated into the model. Before each time step, a uniformly mixed cloud was assumed. The terminal velocity of each drop was calculated on the basis of the data of Gunn and Kinzer (1949), and the loss of drops ( $\Delta n_j$ ) by fallout at the end of the time step was calculated by

$$\Delta n_j = n_j \times \frac{V_j}{d} \times \Delta t. \quad (9)$$

#### 4. RESULTS

##### VERIFICATION OF THE NUMERICAL MODEL

The validity of the numerical model was checked by comparing its predictions with experiments conducted at the Cornell Aeronautical Laboratory (Pilié et al. 1967, Jiusto et al. 1968). These experiments were conducted in a cylindrical chamber 9 m high and 9 m in diameter. Fog was formed on natural aerosol nuclei in the atmosphere by first pressurizing the chamber and then cooling the air by venting the chamber in a controlled manner. No cooling occurred between 8 and 11 min, the period in which seeding was accomplished. Visual range was calculated from measurements of the extinction coefficient obtained with a transmissometer. The seeding agent used was NaCl.

A run using an 8-mg m<sup>-3</sup> NaCl seeding agent having a maximum particle number concentration between 4 and 5  $\mu$ m in diameter is discussed in some detail in the Cornell reports and is used herein as the principal basis of verification of the model. In our numerical experiment, the distribution of the natural aerosols was simulated by means of 27 particle sizes, peaked at 0.1  $\mu$ m in diameter (table 2). The size distribution of seed particles was simulated by five particle sizes (table 3) and approximates the distribution given by Jiusto et al. (1968).

A cooling rate of 4°C hr<sup>-1</sup> from an initial temperature of 24°C was reported by the Cornell experimenters. A

TABLE 2.—Aerosol distributions used in experiments

Diameter of dry nucleus ( $\mu$ m)	0.10 $\mu$ m peak		0.35 $\mu$ m peak
	No. per cm <sup>3</sup> if total = 500 cm <sup>3</sup>	Relative concentration (%)	Relative concentration (%)
0.05	18.59	3.585	0.024
.06	27.89	5.578	.048
.07	37.19	7.438	.097
.08	46.49	9.298	.145
.09	55.78	11.155	.193
.10	74.38	14.875	.242
.12	55.78	11.155	.483
.14	46.49	9.298	.967
.16	37.19	7.438	1.450
.18	27.89	5.578	1.930
.20	18.59	3.718	2.417
.22	9.30	1.860	4.835
.24	8.37	1.674	7.252
.26	7.44	1.488	9.670
.28	6.51	1.302	12.087
.30	5.58	1.116	14.505
.35	4.65	0.930	19.340
.40	3.72	.744	14.505
.50	2.79	.588	4.835
.60	1.86	.372	1.934
.70	0.930	.186	0.967
.80	.837	.167	.483
.90	.744	.149	.242
1.50	.930	.186	1.209
2.50	.0930	.019	0.121
3.50	.00930	.0019	.0121
4.50	.000930	.00019	.00121

TABLE 3.—Seed size distribution used in simulating the Cornell experiment

Diameter of dry seed particles ( $\mu$ m)	Relative concentration (%)
1.0	12.0
2.0	15.0
3.0	14.0
4.0	19.0
5.0	15.0
6.0	10.0
7.0	7.0
8.0	3.0
9.0	5.0

comparison of the laboratory and numerical experiments is shown in figure 8. The reported values of liquid water density within the laboratory-produced fog are considerably smaller than either those predicted in the numerical model or those resulting in adiabatic cooling of 4°C hr<sup>-1</sup> with no fallout of cloud droplets. If the Cornell experiments were made using an expansion rate for which the dry adiabatic cooling rate would be 4°C hr<sup>-1</sup>, the cooling rate with concurrent condensation would be about half that value (because of warming due to heat of condensation). If a cooling rate of 2°C hr<sup>-1</sup> is assumed, the computed liquid water density approximates those measured during the Cornell experiments, and experimental results and numerical calculation are in even closer agreement with respect to visibility and visibility improvement (fig. 9). The distribution of water density between natural and seed particles is shown in figures 8 and 9,

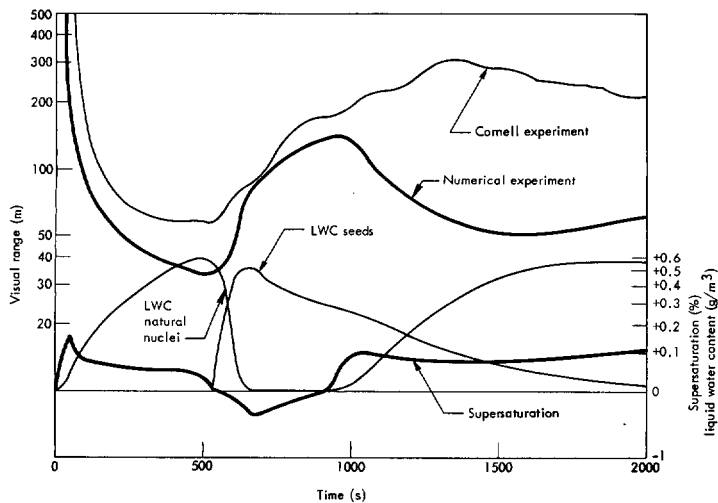


FIGURE 8.—Comparison of the visual (meteorological) range from laboratory data (Cornell Aeronautical Laboratory) with the numerical model; cooling rate,  $-4^{\circ}\text{C hr}^{-1}$ . The lower curves show the trend of supersaturation and liquid water content (LWC). The cloud was 9 m thick.

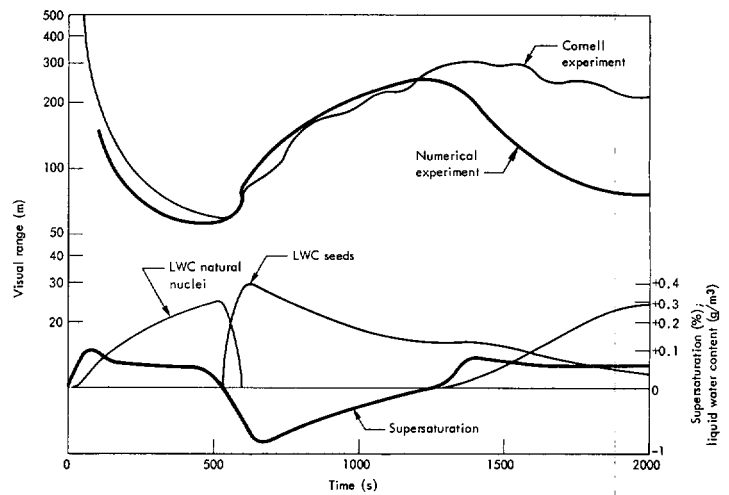


FIGURE 9.—Same as figure 8, except for  $-2^{\circ}\text{C hr}^{-1}$ .

and the change of fog-droplet size distribution with time is shown in figure 10.

Although numerical simulation and laboratory experiment are not in particularly good agreement if the stated  $4^{\circ}\text{C hr}^{-1}$  cooling rate is used in the numerical calculation, there seems to be sufficient justification to compare visibility and visibility-improvement factors under the assumption of a  $2^{\circ}\text{C hr}^{-1}$  cooling rate. If this is done, there is good agreement between laboratory and numerical experiments. If lesser amounts of seeding materials are simulated, visibility improvement decreases in accordance with experimental observations.

Figures 8 and 10 illustrate the characteristic simulated behavior of fog during seeding. Initially, the dry aerosol particles absorb water and become larger; a peak in supersaturation occurs shortly after the relative humidity exceeds 100 percent ( $\sim 50$  s in fig. 8). After this peak supersaturation is reached, the aerosol spectrum can be regarded as dividing itself into two groups: (1) larger aerosols upon which stable fog droplets form and continue to grow and (2) smaller aerosols that cease growing and remain haze-size particles. The latter particles never reach the critical size and supersaturation corresponding to their nucleus content. In the upper left diagram of figure 10, the absence of particles from 1 to  $5\text{ }\mu\text{m}$  in diameter indicates that droplets incorporating natural aerosols segregate into "haze particles" (smaller than  $\sim 3\text{ }\mu\text{m}$ ) and "fog droplets" (larger than  $\sim 3\text{ }\mu\text{m}$ ).

As time passes, both visibility and supersaturation decrease, while fog droplets grow larger and the liquid-water content increases. The number density of drops diminishes slightly, primarily because larger drops tend to fall out. Shortly after seeding ( $\sim 600$  s in figs. 8 and 10), the relative humidity falls below 100 percent; and many of the fog droplets evaporate to the size of haze particles.

Consequently, the liquid-water content of droplets incorporating natural aerosol particles rapidly decreases, while that of seed-containing droplets increases. The total number of fog-size droplets decreases, the spectrum of sizes broadens, and visibility improves. The ability of the seed material to absorb water continually decreases: (1) because the seed-containing droplets become dilute and the vapor density over them approaches that of infinitely dilute droplets and (2) the larger, seed-containing droplets fall out of the fog.

Ultimately, the improvement in visibility reaches a maximum. At this time ( $\sim 900$  s in figs. 8 and 10), the relative humidity has increased to approximately 100 percent; and many of the original aerosol particles are once again growing from haze to fog-droplet size. There is still a broad size-distribution of particles, but many large seed particles have fallen out, removing a significant quantity of water—an important source of visibility improvement.

Visibility continues to decrease as the original aerosol particles grow to fog-droplet size and the number density of droplets increases; once again, most of the liquid-water content of the fog is found in drops containing the original aerosol particles. One can consider the fog as once more established and unaffected by the seeding operation. In the second generation of fog, both a peak supersaturation and a break between haze particles and fog droplets occur, just as during the original formation of fog.

The above sequence of events is similar to that observed in the Cornell experiments, except that the fog is re-established more quickly in the numerical simulation. We conclude that the numerical simulation represents the experimental findings sufficiently well to justify additional numerical experiments and the assessment of ranges of applicability of salt seeding.

Most of the simulation experiments performed with the model incorporated a thermal sequence similar to that of the Cornell experiment: initial cooling from saturation

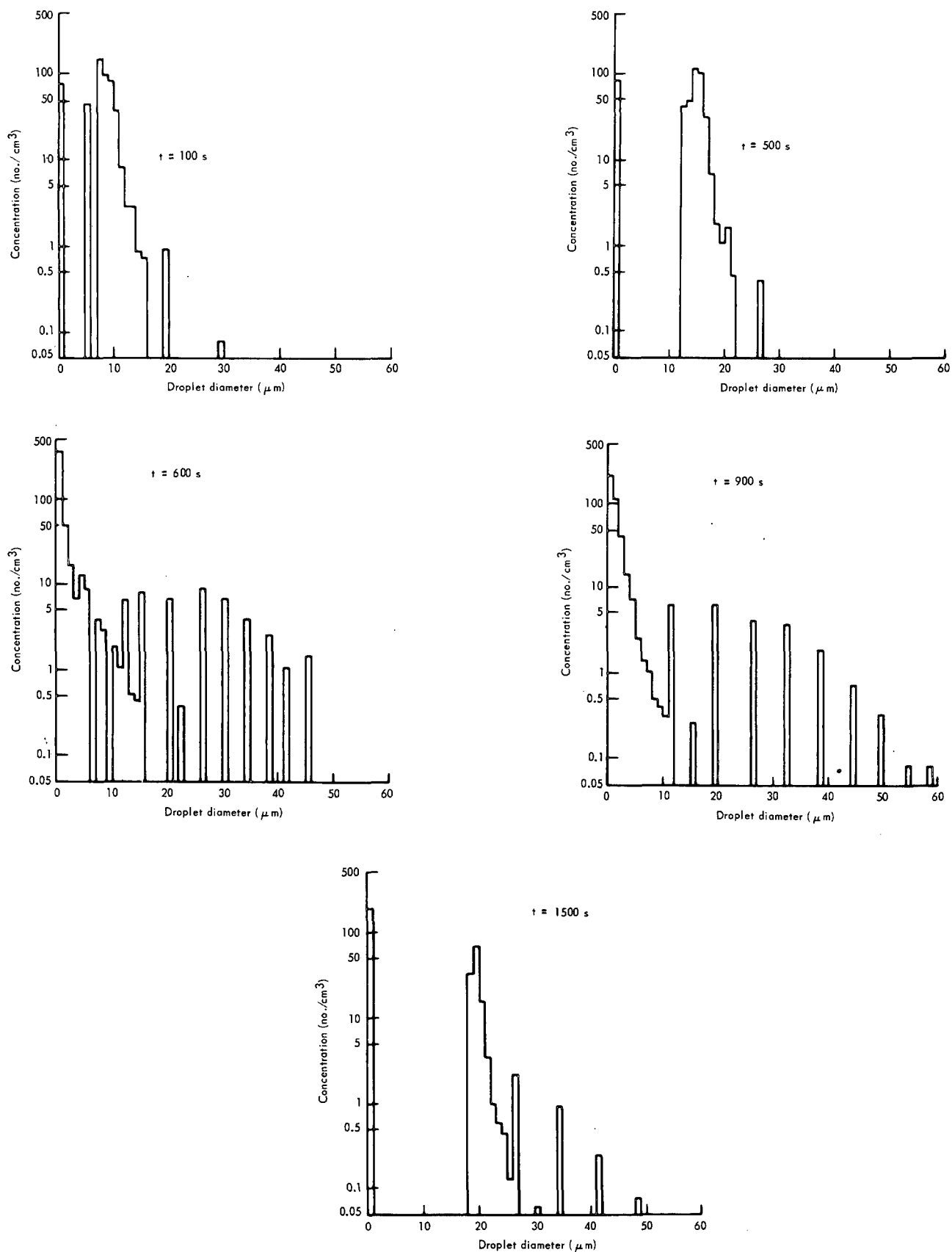


FIGURE 10.—Change in the fog-droplet size distribution with time, predicted by a numerical model using an  $8 \text{ mg m}^{-3}$  NaCl seeding agent and a cooling rate of  $-4^{\circ}\text{C hr}^{-1}$ . The cloud was 9 m thick.

for about 9 min, followed by isothermal seeding for about 3 min, followed by cooling. Hence, conditions conducive to continual fog generation were present after seeding; and visibility improvement underwent subsequent deterioration as the effectiveness of the seeded material declined with time. At present, for outdoor operations, it seems premature to attempt to disperse an actively forming fog, as modeled above. It would be more practical to hasten the departure of a stagnant or slowly dissipating fog.

#### EFFECT OF SEED QUANTITY AND SIZE

The ability of seed material to absorb water is primarily a function of its total mass, and the initial rate at which a given mass of seed material will absorb water is a function of its surface area. On this basis, one would predict that the greater the quantity of seed and the more finely it is ground, the more rapidly water will be transferred from natural to seed particles; and consequently the greater will be the improvement of visibility. This argument, however, is erroneous, for it does not take into account the restriction of visibility caused by new droplets grown on the seed particles or the period of time that a seed particle actively absorbs water at the expense of natural particles.

To minimize the visibility restriction caused by the seeds and to maximize the period of time that the seeds will effectively absorb water, one might suggest using the largest possible seed particles, expecting they would form relatively few but large droplets that would produce a nearly transparent fog. From another point of view, however, one can desiccate natural fog particles more effectively by seeding the same number density of large particles as one might of small particles (because the seed mass is increased). Also of importance is the fact that, if fewer large seed particles are employed, they will grow and fall out more quickly, carrying with them more fog water than if small particles were used. Large particles might fall too rapidly, however, and may fall out of the fog before being utilized efficiently; therefore, one might expect a greater mass of large seed particles to be needed than would be true of smaller seed particles. These expectations are verified in table 4 and figure 11, which summarize the results of calculations and shed light on the effect of seed size and quantity upon visibility improvement. Figure 12 illustrates predicted seeding results using several different quantities of seeds and a constant cooling characteristic, initial aerosol spectrum, and seed size. Similar data from experiments with larger seeds and greater cloud depth are shown in figure 13.

As indicated in table 4, in the case of 80- $\mu\text{m}$  seeds, the predicted visibility improvement is remarkable. Although the general trend depicted in these tables seems reasonable, there are compelling reasons to question the value of the predictions with regard to the larger seeds. The model treats the cloud as being homogeneous, with no relative motion between fog particles and environment.

TABLE 4.—Influence of seed quantity and size on visibility improvement†

Cloud depth (m)	Seed parameter			Visual range			
	Diameter ( $\mu\text{m}$ )	Density ( $\text{mg m}^{-3}$ )	Concentration (no. $\text{cm}^{-3}$ )	Min (m)	Max (m)	Time max (s)	Ratio (max/min)
9	5	2	14.2	33	44	800	1.3
9	5	4	28.3	33	97	900	2.9
9	5	8	56.4	29	160	1110	5.5
9	5	16	112.8	33	160	1402	4.8
9	5	32	225.6	30	162	1830	5.4
90	5	1	7.1	29	34	640	1.2
90	5	2	14.2	29	31	680	1.1
90	5	4	28.3	29	55	920	1.9
90	5	8	56.4	29	52	680	1.8
90	10	8	7.1	28	63	940	2.2
90	10	12	10.6	29	100	1300	3.4
90	10	16	14.2	29	97	1500	3.3
90	10	27	24.0	29	91	2000+	3.1+
90	10	32	28.3	28	93	2290	3.3
90	20	16	1.8	28	46	810	1.6
90	20	32	3.5	29	256	1150	8.8
90	20	64	7.0	29	307	1680	10.6
90	20	128	14.1	28	340	2120	12.1
90	40	32	0.44	29	49	760	1.7
90	40	64	.88	29	373	960	12.8
90	40	128	1.76	28	1480	1383	50.3
90	80	32	0.055	29	31	670	1.1
90	80	64	.110	28	35	733	1.2
90	80	128	.221	28	66	780	2.4
90	80	256	.441	28	2926	1110	100.5
90	80	512	.884	29	24700	1490	850.0†

†All experiments with 500 aerosol particles per cubic centimeter and a peak concentration at a 0.1- $\mu\text{m}$  diameter; the cooling rate was  $4^{\circ}\text{C hr}^{-1}$ .

‡See the comment in section 4 under the heading "Effect of Seed Quantity and Size."

The vapor-density field surrounding each particle is assumed unaffected by other particles, and Laplace's equation is assumed valid. At the peak in visual range predicted for seeding 512  $\text{mg m}^{-3}$  of 80- $\mu\text{m}$  seeds, the seeds have grown to 230  $\mu\text{m}$  in diameter, and most have fallen out of the cloud, carrying the fog water with them. Only about 300 seed particles per cubic meter remain. The terminal velocity of the remaining particles is high enough to require the use of a ventilation factor in calculating their growth, and it is questionable whether such a small number of falling particles would have other than a local effect on the vapor density. It should also be borne in mind that there is a practical limit to the mass density of seed material that can be economically dispersed or that, after fallout to the ground, would give a permissible level of pollution. The latter, of course, would be a function of the chemical composition of the seeds.

Figure 14 contains data on the effectiveness of 4- and 5- $\mu\text{m}$  seed particles. Equal masses (8  $\text{mg m}^{-3}$ ) of seed material were simulated in these experiments; consequently, more than twice as many 4- $\mu\text{m}$  as 5- $\mu\text{m}$  seeds were required to maintain a constant initial mass density. The concentration of 4- $\mu\text{m}$  seeds (120  $\text{cm}^{-3}$ ) is relatively large, and hence the seed-containing droplets significantly decrease visibility. There are so many 4- $\mu\text{m}$  seeds

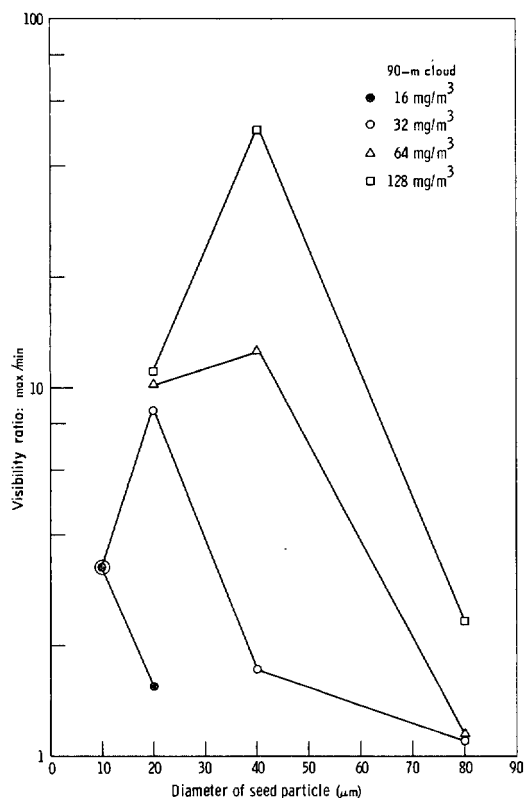


FIGURE 11.—Ratio of the maximum visual range achieved after seeding to the visual range prior to seeding in the case of fog having an active fog-producing mechanism present.

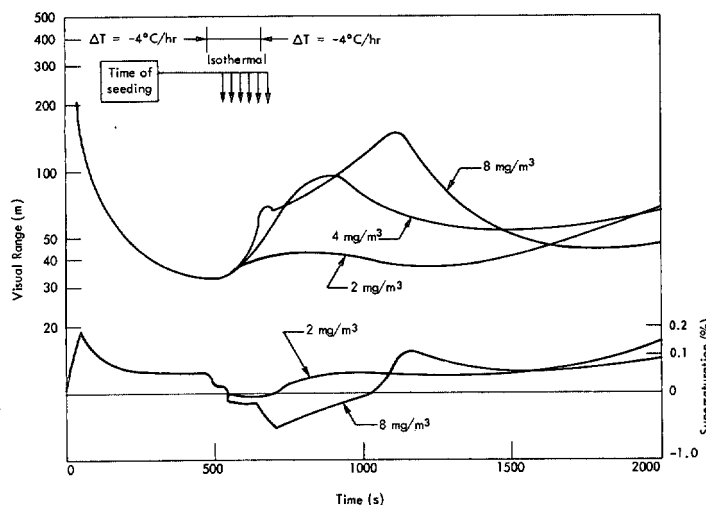


FIGURE 12.—Comparison of the predicted change in the visual (meteorological) range with time, using several seeding rates. The seed particles are  $5\text{ }\mu\text{m}$  in diameter; the original aerosol contained 500 particles per cubic centimeter peaked at a  $0.1\text{-}\mu\text{m}$  diameter; the cooling rate was  $-4^\circ\text{C hr}^{-1}$ . The cloud was 9 m thick.

that they do not grow quickly. Consequently, they fall out of the cloud slowly; and visibility only improves slowly. It is of interest to note that, for the  $4\text{-}\mu\text{m}$  seeds, the water vapor density remains below saturation for a longer period of time and attains lower values than for  $5\text{-}\mu\text{m}$  seeding. This is a direct consequence of the fact that a greater mass of seed material remains in the  $4\text{-}\mu\text{m}$

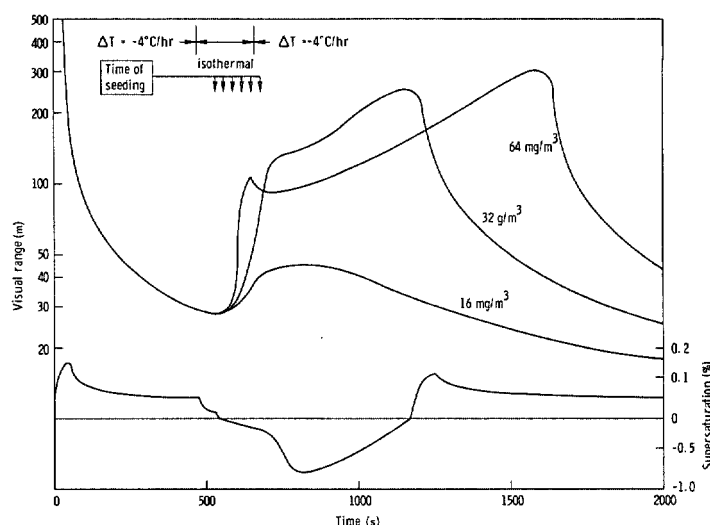


FIGURE 13.—Comparison of the predicted change in visual (meteorological) range with time, using a constant seed diameter ( $20\text{ }\mu\text{m}$ ), and with three different mass concentrations. The original aerosol contained 500 particles per cubic centimeter peaked at a  $0.1\text{-}\mu\text{m}$  diameter. The cloud was 90 m thick. The lower curve is the trend of supersaturation for a  $32\text{ g m}^{-3}$  dose.

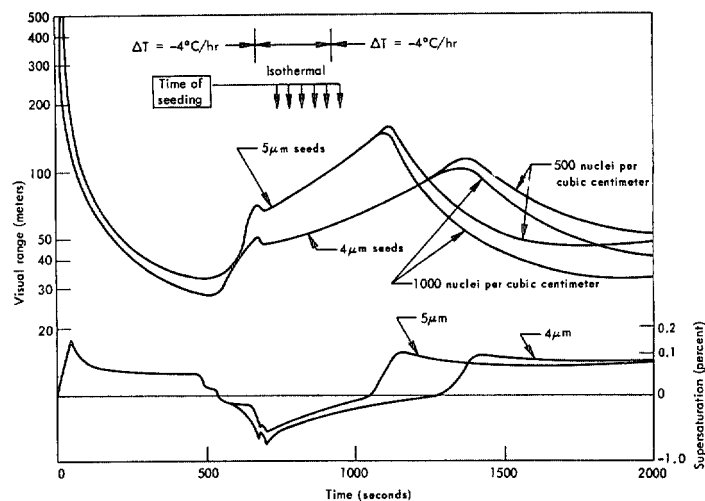


FIGURE 14.—Comparison of the predicted change in the visual (meteorological) range with time, using original air having various aerosol contents and using constant seed mass concentrations ( $8\text{ mg cm}^{-3}$ ) but different sizes and, consequently, different number concentrations. The aerosol concentration peaked at a  $0.10\text{-}\mu\text{m}$  diameter. The cloud was 9 m thick.

seeded fog as a result of the slower growth and lower terminal velocity of the droplets grown on the large number of seed particles. Seeds much smaller than  $4\text{ }\mu\text{m}$  are expected to be ineffective.

Figure 15 contains data similar to those of figure 14, except that much larger seeds have been simulated. In the illustrated experiments,  $32\text{ mg m}^{-3}$  of seed material were simulated. Significant clearing is predicted for  $20\text{-}\mu\text{m}$  seeds, but very little for  $40\text{-}\mu\text{m}$  seeds [and virtually none for  $80\text{-}\mu\text{m}$  seeds (not shown)]. In these cases, the absence of clearing for large seeds is related to their rapid growth, fallout, and consequent low number density and inability to absorb water rapidly from the cloud.

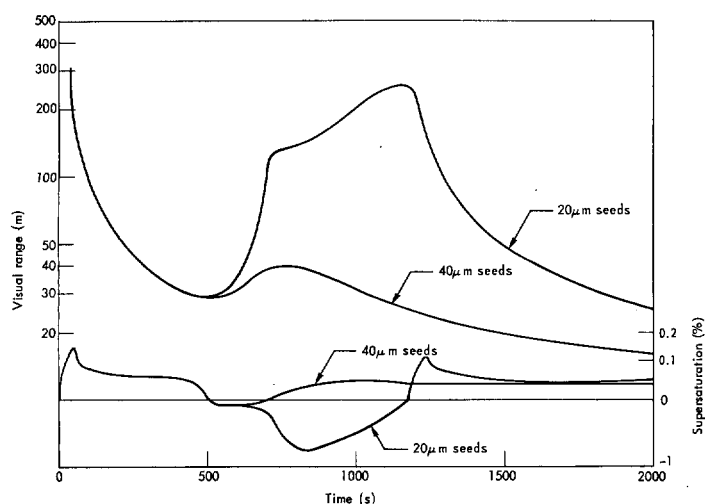


FIGURE 15.—Comparison of the predicted change in visual (meteorological) range with time, using constant seed mass concentrations but different sizes and, consequently, different number concentrations. The original aerosol contained 500 particles per cubic centimeter peaked at a  $0.10\text{-}\mu\text{m}$  diameter. The cloud was 90 m thick; the cooling rate was  $-4^{\circ}\text{C hr}^{-1}$ .

A comparison of figures 14 and 15 emphasizes the fact that the proper mass concentration of seeds is dependent on size.

Outdoor visibility-improvement operations will be hampered by atmospheric motions that are not considered in these numerical experiments. Generally, the seeded volume will be transported by the ambient wind and mixed with untreated foggy air. The shorter the period of time between seeding and achievement of the desired visibility change, the easier will be the targeting problem posed by any ambient wind, and also the less the treated volume will be diluted by turbulent mixing with untreated air. These considerations suggest the use of large seed particles; for as shown in figure 16, the larger the seed particle, the more quickly clearing is effected. Evidence such as that shown in figure 11 suggests that the maximum obtainable clearing becomes an increasingly strong function of initial seed concentration (at least up to  $40\text{-}\mu\text{m}$  seeds). However, large seeds necessitate large mass dispersal; and while the tolerable level of salt contamination varies with circumstances, it seems clear that seeds larger than about  $50\text{ }\mu\text{m}$  in diameter will require intolerable masses—viewed either as a dispersal or ground contamination problem.

#### EFFECT OF DIFFERENCES IN FOG THICKNESS

Fog thickness influences the numerical prediction because of its effect on the period of time that a drop or seed particle remains in the fog. Three thicknesses of fog were simulated: 9 m, 90 m, and infinite. The first might be applicable to radiation fogs, but it was chosen primarily to predict what might occur in the Cornell Laboratory chamber under various circumstances; the second was chosen to simulate more common natural-fog situations; and the last, to remove the effects of drop fallout. Fallout

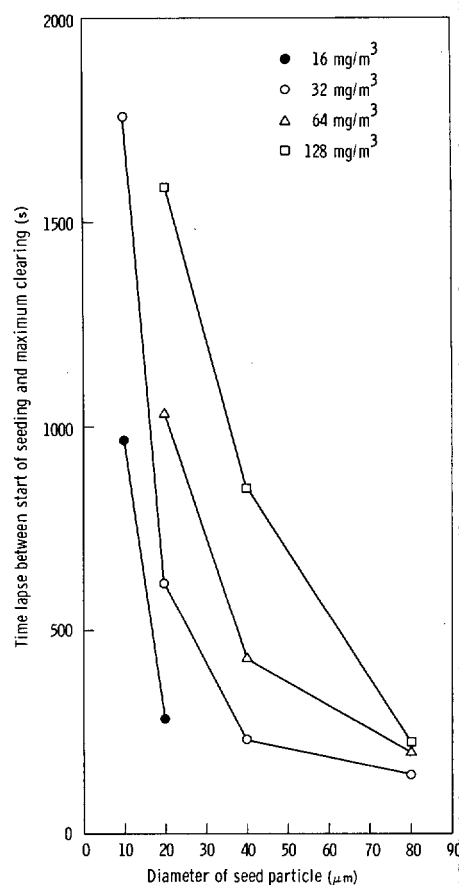


FIGURE 16.—Time lapse between the start of seeding and the period of maximum clearing as a function of seed particle size and quantity in the case of a 90-m cloud having a cooling rate of  $-4^{\circ}\text{C hr}^{-1}$ .

was simulated by subtracting from the total number of droplets, for each size, the number of drops present, multiplied by the distance they would fall during the time step, divided by the thickness of the cloud. Thus, in effect, the cloud was assumed homogeneous before each time step. Therefore, even after the first time step, a few drops were assumed to fall out; and even if, for a certain size category, the sum of the fall distance during several time steps exceeded the thickness of the fog, some drops would remain.

If seed particles fall through the fog before their full potential to absorb water is realized, they are inefficiently utilized; and a large amount of seed material is required. If, on the other hand, the fog is so thick (or the seed so small) that seed particles remain after they become, in effect, infinitely dilute, the seed loses much of its potential as a fog-clearing agent. Visibility is improved solely as a result of the redistribution of the water content of the fog from many to fewer droplets, and the potentially greater effects of removing water content by fallout are only slowly, if ever, realized.

The period of effectiveness of a seed particle is a function of its size and of the water-vapor density of the environment to which it is exposed. The latter factor is a function of the mass of seed material employed and the degree of activity of the fog-producing process. On the

TABLE 5.—Influence of cloud depth on visibility improvement†

Cloud depth (m)	Seed parameter		Visual range			
	Diameter ( $\mu\text{m}$ )	Density ( $\text{mg m}^{-3}$ )	Min (m)	Max (m)	Time max (s)	Ratio (max/min)
Infinite	5	8	29	47	690	1.6
90	5	8	29	52	680	1.8
9	5	8	29	160	1110	5.5
90	5	4	29	54	920	1.9
9	5	4	33	92	900	2.8
90	10	16	29	97	1500	3.3
9	10	16	35	631	931	18.0
90	20	32	29	257	1150	8.9
9	20	32	35	250	761	7.2
90	40	64	29	373	960	12.8
9	40	64	35	69	721	2.0
90	80	512	29	24700	1490	850.0
9	80	512	35	421	741	12.0

† All experiments were with 500 aerosol particles per cubic centimeter and a peak concentration at a  $0.1\text{-}\mu\text{m}$  diameter; the cooling rate was  $4^\circ\text{C hr}^{-1}$ .

basis of computed results (e.g., figs. 8, 9, and 12), we conclude that the duration of effectiveness is approximately the period in which the ambient vapor density is below saturation.

Table 5 summarizes the results of several experiments bearing on the effect of fog thickness on seedability. It is apparent that seed particles  $5\text{ }\mu\text{m}$  in diameter could be used to improve the visibility in a 9-meter-thick fog, but would be of little value in a fog 90 m or greater in thickness. The thicker fog requires larger particles and a greater mass of seeding material per unit volume. Relatively large particles can be used for seeding thin clouds. If particles are larger than "optimum" size, fewer are needed; but there must be a greater mass per unit volume.

A factor not adequately accounted for in the numerical experiment is the time over which a particular volume of fog is exposed to seed particles. Large, rapidly falling particles may fall through a particular volume too quickly for significant amounts of water vapor to diffuse from fog droplets to seed particles. In this case, clearing would be less than predicted, as the experiment assumes homogeneous mixing.

#### EFFECTS OF VARIATIONS IN RAPIDITY OF DISPERSAL

For approximating the conditions of the Cornell experiment, seed materials were generally introduced in six lots, each separated by 30 simulated seconds. In a few cases, all seed material was introduced at once; and in a few others, seeding was extended over longer periods. In general, one batch of seed material lowers the value of the minimum water-vapor density but maintains subsaturation for a shorter period of time than does multi-batch seeding. Results generally indicate that, if all seed material is introduced before the time of maximum clearing for single-dose seeding, there is little difference in the effectiveness of single- and multiple-dose seeding. When the total seeded mass concentration is identical in both

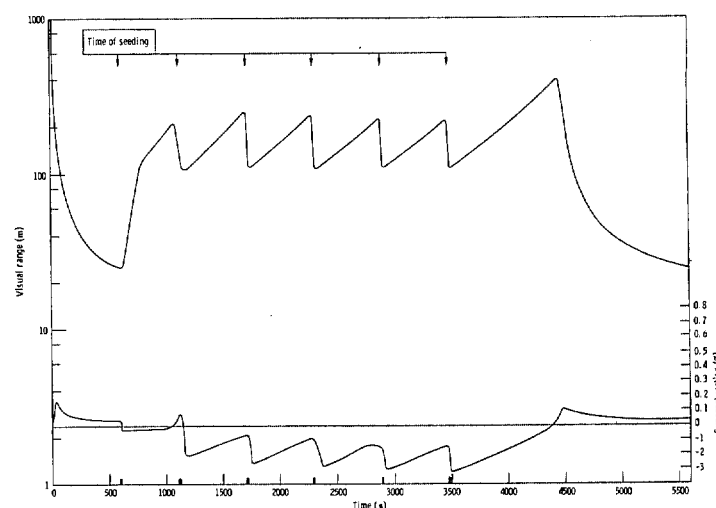


FIGURE 17.—Trend of visual range with time in the case of a 90-meter-thick fog treated repeatedly with seed particles.

cases, there is less visibility improvement if seeding continues beyond the time of maximum clearing for a single dose.

Figure 17 illustrates results of periodically seeding an active fog. A cooling rate of  $4^\circ\text{C hr}^{-1}$  continued throughout the experiment; six batches of seeds were introduced into the fog, the first after 600 s and the others at intervals of about 600 s thereafter. A mass concentration of  $32\text{ mg m}^{-3}$  of 20-micrometer-diameter seed particles was used for each batch of seeds. Results using the same mass concentration under the more commonly used conditions of the Cornell experiment are shown in figure 13. In principle, it appears that an effective way of maintaining improved visibility within an air mass containing an active fog-producing mechanism would be to periodically inject the air mass with large seeds that fall out before a succeeding batch is introduced.

Slow seeding by relatively small seed particles is ineffective because seed particles having a low mass density cannot absorb sufficient fog water to significantly lower the water vapor density below saturation; consequently, the evaporation of natural fog droplets is insufficient to cause much visibility improvement. Furthermore, some of the seeds themselves grow large enough to behave like infinitely dilute droplets, and are indistinguishable from natural fog droplets with regard to their ability to absorb water. Continued or periodic seeding only has merit if a new volume of air is, in fact, treated, or if the seed particles are sufficiently large so that the droplets formed upon them fall out of the fog.

#### EFFECT OF DIFFERENCES IN NATURAL AEROSOL CONCENTRATION AND SIZE DISTRIBUTION

Natural aerosols in the atmosphere were modeled, using input parameters for 27 different sizes of NaCl particles (table 2). Numerical experiments were made

TABLE 6.—*Influence of initial aerosol concentration on visibility improvement†*

Aerosol concentration	Seed parameter		Visual range			
	Diameter ( $\mu\text{m}$ )	Density ( $\text{mg m}^{-3}$ )	Min (m)	Max (m)	Time max (s)	Ratio (max/min)
250	5	8	45	176	1140	3.9
500	5	8	29	160	1110	5.5
1,000	5	8	29	142	1090	4.9
10,000	5	8	23	75	990	3.2

†All experiments were conducted using an aerosol size distribution peaking at a diameter of  $0.1 \mu\text{m}$  and a cooling rate of  $4^\circ\text{C hr}^{-1}$ .

using aerosol particle concentrations ranging from 250 to 10,000 particles per cubic centimeter with constant relative concentration, the mode aerosol diameter being  $0.1 \mu\text{m}$ . Results of experiments using 500 and 1000 nuclei per cubic centimeter and two different seed dosages are shown in figure 14. A comparison of results using concentrations of 500, 1,000, and 10,000 particles per cubic centimeter indicates that minimum visual ranges were equal before seeding and that maximum visual range increases with decreasing aerosol content. This suggests that fog formed in a "clean" atmosphere is more susceptible to artificial modification than fog formed in a "dirty" atmosphere. As shown in table 6, however, the differences are not remarkable; and in a field effort, it is doubtful whether the aerosol content of the air will detectably influence its seedability.

Results with an aerosol concentration of 250 particles per cubic centimeter reversed this trend. Although a greater maximum visual range was achieved in "seeding" this fog, the minimum visual range was 50 percent greater than in the other three cases; and the overall percentage improvement was less. The greater minimum visual range resulted from the fact that, when the fog is composed of fewer droplets, they grow more rapidly than do droplets when the concentration of aerosols is higher. Greater supersaturations occur in fogs formed in relatively clean air due to the absence of sufficient large aerosol particles and the consequent necessity to activate relatively small ones. This leads to more rapid growth of those droplets that are formed. Since, for a given fog water content, the visual range is proportional to the mean diameter of the droplets, the natural fog formed in clean air is more transparent than that formed in dirty air. This effect may be somewhat overstated in the numerical prediction, which reflects a discontinuous size distribution of aerosols.

The use of an aerosol concentration of  $10,000 \text{ cm}^{-3}$  does not result in an absurdly large number of fog droplets. At the time of minimum visual range, there are 200 droplets  $10 \mu\text{m}$  or larger in diameter and 1,000 larger than  $5 \mu\text{m}$ . If an aerosol concentration of  $1000 \text{ cm}^{-3}$  is used, there are 400 droplets  $10 \mu\text{m}$  or larger in diameter and 500 larger than  $5 \mu\text{m}$ .

Numerical experiments were made using two different aerosol size distributions having mode diameters of  $0.1$

TABLE 7.—*Influence of initial aerosol size distribution on visibility improvement†*

Aerosol spectrum‡	Seed parameter		Visual range			
	Diameter ( $\mu\text{m}$ )	Density ( $\text{mg m}^{-3}$ )	Min (m)	Max (m)	Time max (s)	Ratio (max/min)
0.35	5	8	32	116	1050	3.6
.10	5	8	29	160	1110	5.5
.35	5	4	32	88	860	2.7
.10	5	4	33	97	900	2.9
.35	5	2	32	42	800	1.3
.10	5	2	33	44	800	1.3
.35	4	8	32	86	1330	2.7
.10	4	8	34	116	1380	3.4

†All experiments were with 500 aerosol particles per cubic centimeter and a cooling rate of  $4^\circ\text{C hr}^{-1}$ .

‡The number refers to size (in micrometers) of the modal value of aerosol in the spectrum; see table 2 for a comparison among the spectra used.

and  $0.35 \mu\text{m}$ , respectively (table 7). Everything else being the same, fog formed in the air mass having the smaller mode-size aerosol was found to be the more susceptible to seeding. The difference occurred predominantly in the maximum visual range achieved after seeding, rather than in the minimum visual range before seeding.

#### EFFECT OF MONODISPersed SEED PARTICLES IN CONTRAST TO THAT OF POLYDISPersed SEED PARTICLES

For examining the influence of seed size, seeding was simulated in most of the numerical experiments by means of monodispersed seed particles. To simulate the Cornell experiments, several experiments were made using a polydispersed seed. A comparison of the results achieved (cf. figs. 8 and 14) indicates that, whereas the maximum visibility improvement may be similar in both cases, the period of time during which visibility remains near the maximum is considerably shorter for monodispersed seeds than for polydispersed seeds. This suggests that monodispersed seed particles are not ideal, and a distribution of seed sizes appears more desirable.

#### EFFECT OF DROPLET FALLOUT

The initial improvement in visibility in a seeded fog results from the redistribution of the water content from the many natural droplets toward the artificially produced droplets. Because of their large nuclei, these seed-produced droplets grow relatively large and typically attain appreciable terminal velocities relative to droplets containing natural nuclei. Visibility is improved by the fallout of the seed particles, which remove liquid water from the fog. If the fog-forming process stops, the visibility improvement should be more or less permanent (neglecting turbulent mixing with untreated, foggy air). In our experiments, the fog-forming process continued after seeding was simulated. As a result, after seed-containing droplets had substantially fallen out, condensation once more occurred on the natural fog droplets; and visibility again decreased. During the period in which seed particles

are effective, the water-vapor density falls below saturation; and the subsequent rise of vapor density above saturation signals the end of the effectiveness of the seed particles and serves as a harbinger of lower visibility. This sequence of events is graphically shown on many of the figures (e.g., fig. 8).

#### EFFECT IF FOG-FORMING PROCESS IS NOT OPERATING

If a fog-forming process is not operating and no mixing of seeded and nonseeded fog volumes is permitted, one would expect continued fog clearance as a result of the loss of water content in the fog as droplets fall out. Seeding would hasten the process if the seeds grew larger and fell out faster than the natural fog droplets. At present, there is little prospect of clearing an actively growing fog such as those that generally have been modeled in this work.

It is useful to contrast the predicted behavior of a growing fog with a static one under similar seeding conditions. This is done in figure 18. The two fogs depicted in figure 18 have common histories until 2480 s: a 480-s growth period in which the temperature decreases at a rate of  $-4^{\circ}\text{C hr}^{-1}$ , followed by a 2000-s ripening period during which the temperature remains constant, the drops adjust their sizes to approach equilibrium conditions, and some water content is lost because of droplet fallout. Commencing at 2480 s, both fogs are seeded, one with a single batch of seed particles and the other with the more usual six batches of seeds, each separated by 30 s (however, a total of  $32\text{ mg m}^{-3}$  of 20-micrometer-diameter seeds was simulated in both instances). Also commencing at 2480 s, the thermal characteristics of the fogs diverge; the multibatch seeded fog remains isothermal while the single-batch seeded fog is once again subjected to a cooling rate of  $-4^{\circ}\text{C hr}^{-1}$ .

The general behavior of the two fogs is similar for approximately 700 s following the initial introduction of seeds. In the static-fog case, about 80 percent of the seeds have fallen from the fog by this time (about 3200-s total elapsed time in fig. 18). The remainder, whose growth rate has markedly slowed, are dilute drops approximately  $82\text{ }\mu\text{m}$  in diameter. At the end of another 10 min, the seeds have increased their diameter only about  $1\text{ }\mu\text{m}$  and are essentially in equilibrium with the environment. The vapor density in the cloud remains nearly constant at a value about 98 percent of saturation. After the initial shrinkage of the natural fog droplets in the first few hundred seconds after seeding, visibility improvement is largely a result of the reduced water content of the fog caused by the fallout of seed-containing droplets. In figure 18, three stages in the metamorphosis of a seeded, inactive fog can be identified: (1) ripening of droplets (cloud droplets adjust their sizes toward equilibrium with the environment, and the liquid water content of the fog gradually decreases as a consequence of droplet fallout); (2) seeding and rapid growth of seed particles (visibility increases markedly, primarily due to the modification of the droplet spectrum as a consequence of the evaporation of many natural droplets and the creation of few artificial droplets); and (3) moderate growth and

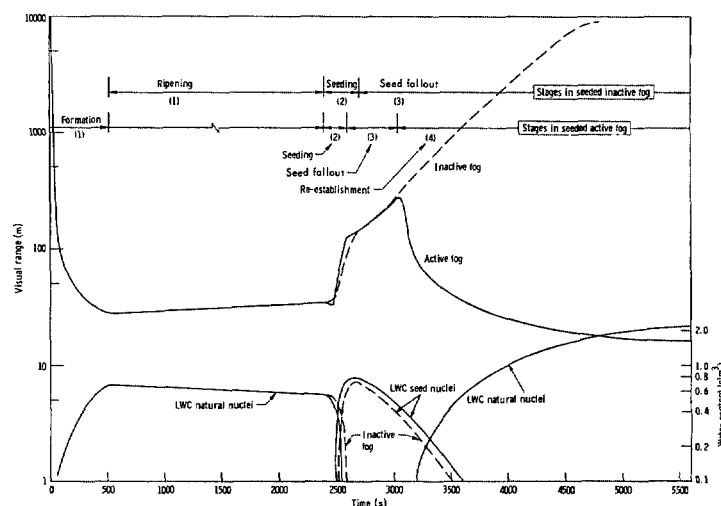


FIGURE 18.—Comparison between certain characteristics of fogs with and without an active fog-producing mechanism present.

fallout of seed particles (visibility increases less rapidly, and improvement becomes increasingly dependent upon the decrease in liquid-water content of the fog as seed-containing droplets fall out and less dependent upon changes in the droplet spectrum).

In the actively forming fog, the seed particles continuously grow, being fed by the vapor being made available by the cooling of the environment. About 80 percent of the seeds have fallen out 700 s after their initial introduction, and the remainder are over  $100\text{ }\mu\text{m}$  in diameter. The drops are quite dilute; and consequently, their growth rate has slowed. This, together with their low concentration, makes it increasingly difficult for the seed particles to absorb the water being made available for condensation. As a result, the relative humidity increases, the natural fog nuclei once again become activated, and the fog re-establishes itself. Figure 18 identifies four stages in the history of a seeded active fog: (1) formation (visibility decreases as condensation on natural nuclei occurs); (2) seeding and rapid growth of seed particles (visibility rapidly improves as a result of redistribution of fog water content); (3) moderate growth and fallout of seed particles (seeds are able to absorb water made available by condensation, and humidity remains below saturation; but visibility improvement is mainly the result of droplet fallout and the reduction of water content of the fog); and (4) re-establishment of natural fog (humidity rises above saturation, there being too few seed-containing droplets to absorb the water being made available by condensation; and the growth of natural nuclei once more commences).

## 5. CONCLUSIONS

The numerical model of fog microphysics used in this study supports the following generalizations:

1. Visibility within fogs can in principle be usefully improved by seeding with condensation nuclei.
2. The greater the mass density of seed particles, the greater will be their effectiveness in evaporating natural fog droplets and reducing their ability to restrict visibility.

3. The greater the number density of seed particles, the greater will be the number density of fog particles formed upon seed material, and consequently the greater will be the reduction in visibility caused by the seed particles themselves.

4. When one attempts to maximize the transparency of fog, the visibility restriction due to both natural and artificial fog particles must be considered. Large quantities of seed material may reduce the undesirable effects of natural-fog particles, but may constitute an even greater source of visibility restriction.

5. For a given mass density of seeds, the larger the seed particles, the more quickly clearing occurs. The use of larger particles, however, does not necessarily produce greater visibility.

6. A properly chosen monodispersed seeding material will produce maximum clearing, but the visibility remains high for a shorter period of time than that achieved by use of a properly chosen polydispersed material. The latter seems preferable to allow variation in translation of a cleared volume to the desired location and to allow useful time to accomplish the mission whose undertaking instigated the seeding.

7. The thickness of the fog to be cleared is a factor to be considered in choosing seed material, particularly if the smallest possible seeds are desired. During their fall through a fog, seed particles must be able to absorb water at the expense of natural particles throughout the period of fall. In a thick fog, in which the time of fall from seed level to the base of the fog is longer than in a thin fog, seed particles must thus be larger.

8. Seed particles between about 20 and 50  $\mu\text{m}$  in diameter are appropriate for seeding fog about 100 m thick. Thin fogs may be cleared more economically with smaller particles, but a lower limit of about 5  $\mu\text{m}$  in diameter for fogs less than 10 m thick is indicated.

9. Seeding material should exclude particles smaller than 5  $\mu\text{m}$  in diameter. Particles larger than about 80  $\mu\text{m}$  in diameter are not detrimental to clearing, but are not economically utilized.

10. The microphysical properties of the natural fog, drop size distribution, drop concentration, and aerosol concentration have secondary, minor influences on the effectiveness of fog seeding.

The present numerical work should be useful as a guide for field experimentation in warm-fog suppression. Since, however, we have attempted to model neither the real atmosphere nor plausible dispersal characteristics of seeding systems, some interpretation is necessary to translate the numerical work to field applications. In particular, we have made no attempt to account for the ambient horizontal wind or the mixing of seeded and unseeded portions of the fog. Although such mixing will initially help to disperse the seed materials properly, later mixing will destroy the clearing achieved. It seems probable that the greater the mixing within the fog and the greater the ambient wind, the faster one would want to achieve clearing. This suggests the use of large seed particles and high mass concentration.

#### ACKNOWLEDGMENTS

This work was supported by the U.S. Air Force under Project RAND, Contract No. F44620-67-C-0045, and by the Advanced Research Projects Agency under Contract No. DAH C15-67-C-0150.

#### REFERENCES

- Fletcher, Neville H., *The Physics of Rainclouds*, Cambridge University Press, England, 1962, 386 pp.
- Gunn, Ross, and Kinzer, Gilbert D., "The Terminal Velocity of Fall For Water Droplets in Stagnant Air," *Journal of Meteorology*, Vol. 6, No. 4, Aug. 1949, pp. 243-248.
- Justo, James E., Pilié, Roland J., and Koemond, Warren C., "Fog Modification With Giant Hygroscopic Nuclei," *Journal of Applied Meteorology*, Vol. 7, No. 5, Oct. 1968, pp. 860-869.
- Koenig, L. Randall, "Numerical Modeling of Condensation," *Research Memorandum RM-5553-NSF*, The Rand Corporation, Santa Monica, Calif., Aug. 1968, 43 pp.
- Koenig, L. Randall, "Numerical Experiments Pertaining to Warm-Fog Suppression," *Research Memorandum RM-6159-PR*, The Rand Corporation, Santa Monica, Calif., Oct. 1969, 49 pp.
- List, Robert J., *Smithsonian Meteorological Tables*, The Smithsonian Institution, Washington, D.C., 1966, 527 pp.
- Middleton, William E. K., *Vision Through the Atmosphere*, University of Toronto Press, Canada, 1952, 250 pp.
- Murray, F.W., "On the Computation of Saturation Vapor Pressure," *Journal of Applied Meteorology*, Vol. 6, No. 1, Feb. 1967, pp. 203-204.
- Pilié, Roland J., Koemond, Warren C., and Justo, James E., "Warm Fog Suppression in Large-Scale Laboratory Experiments," *Science*, Vol. 157, No. 3794, Sept. 15, 1967, pp. 1319-1320.

[Received April 15, 1970; revised June 22, 1970]